

On the use of infrared thermography for monitoring a vial freeze-drying process

*Original*

On the use of infrared thermography for monitoring a vial freeze-drying process / Lietta, Elena; Colucci, Domenico; Giovanni, Distefano; Fissore, Davide. - In: JOURNAL OF PHARMACEUTICAL SCIENCES. - ISSN 0022-3549. - STAMPA. - 108:(2019), pp. 391-398. [10.1016/j.xphs.2018.07.025]

*Availability:*

This version is available at: 11583/2711307 since: 2020-01-07T16:54:54Z

*Publisher:*

Elsevier

*Published*

DOI:10.1016/j.xphs.2018.07.025

*Terms of use:*

This article is made available under terms and conditions as specified in the corresponding bibliographic description in the repository

*Publisher copyright*

Elsevier postprint/Author's Accepted Manuscript

© 2019. This manuscript version is made available under the CC-BY-NC-ND 4.0 license  
<http://creativecommons.org/licenses/by-nc-nd/4.0/>. The final authenticated version is available online at:  
<http://dx.doi.org/10.1016/j.xphs.2018.07.025>

(Article begins on next page)

## **On the use of IR thermography for monitoring a vial freeze-drying process**

Elena Lietta<sup>1</sup>, Domenico Colucci<sup>1</sup>, Giovanni Distefano<sup>2</sup>, Davide Fissore<sup>1,\*</sup>

1. Dipartimento di Scienza Applicata e Tecnologia, Politecnico di Torino,

Corso Duca degli Abruzzi 24, 10129 Torino, Italy

2. IMC Service S.r.l., Via Macello 18, 95030 Mascalucia CT, Italy

---

\* *Corresponding author*  
email: [davide.fissore@polito.it](mailto:davide.fissore@polito.it)  
tel: 0039-011-0904693

## **Abstract**

Monitoring a vial freeze-drying process without interfering with product dynamics is a challenging issue. This paper presents a novel device constituted by an IR camera designed to be placed inside the drying chamber, able to monitor the temperature of the vials, very close to that of the product inside. By this way it is possible to estimate the ending point of the primary drying, the heat transfer coefficient to the product ( $K_v$ ) and the resistance of the dried product to vapour flux ( $R_p$ ). Experiments were carried out in a pilot-scale freeze-dryer, processing 5% and 10% sucrose solutions at different values of shelf temperature and chamber pressure, using both thermocouples and the IR camera to track product dynamics. Results evidence that the measurements (of temperature) and the estimates (of the ending point of the main drying and of  $K_v$  and  $R_p$ ) obtained using the two systems are very close, thus validating the IR camera as an effective PAT for the freeze-drying process. Besides, it was shown that the presence of the IR camera in the chamber is not responsible for any additional heating to the product, and that monitored vials are representative of the majority of the vials of the batch.

## **Keyword**

Freeze-drying, monitoring, IR camera, temperature, sensor, Process Analytical Technology.

## Introduction

Freeze-drying stands out as the most suitable way of stabilizing pharmaceutical and biopharmaceutical products that are poorly stable when formulated as liquid solutions. This is due to the fact that the liquid solvent, water in most cases, that can mediate several drug degradation pathways, may be removed at low temperature without jeopardizing the quality of the product.<sup>1-4</sup> In fact, in a freeze-drying process the liquid product, usually poured into glass vials, is loaded onto the shelves of a drying chamber where, at first, the liquid is frozen and, then, the sublimation of the frozen solvent (primary drying) is obtained by reaching proper values of pressure in the chamber, and supplying heat to the frozen product since sublimation is an endothermic process. Finally, the desired value of residual moisture in the product is obtained by further modifying the operating conditions in the chamber to promote the desorption of the “free water” (secondary drying), i.e. the amount of water that did not turn into the frozen state during freezing and remained bounded to product molecules. Secondary drying is usually attained by further increasing the temperature of the product. With respect to chamber pressure, its value can be decreased to the lowest value that can be attained in the apparatus, or it is maintained at the same value used during the primary drying stage (or even at a higher value, aiming to promote the heat transfer), as it was demonstrated that no significative effect on secondary drying could be observed when increasing the pressure up to a certain level (e.g. 200 mTor, when processing mannitol, moxalactam di-sodium and povidone).<sup>5</sup>

It is well known to every freeze-drying practitioners that product quality in the final product is not jeopardized only in case product temperature remains below a threshold value throughout the drying process, being this threshold dependent on the specific product processed. In most cases, when processing amorphous products, the threshold temperature is the value resulting in the collapse of the dried product (see, among the others, Refs.<sup>6-11</sup>),

although quite often the glass transition temperature is considered, in a precautionary way, as this may result into higher values of residual moisture in the product, a higher reconstitution time, a longer-lasting process and, in some cases, drug degradation. When processing crystallizing products, the threshold value is the eutectic temperature, to avoid the formation of a liquid phase in the system. Besides, additional constraints arise from the design of the equipment. The condenser capacity has to be compatible with the rate of sublimation and choking flow in the duct connecting the chamber to the condenser has to be avoided as both would result into an uncontrolled increase of pressure in the drying chamber, being this responsible for product overheating.<sup>12,13</sup>

In this framework, the "Guidance for Industry PAT - A Framework for Innovative Pharmaceutical Development, Manufacturing, and Quality Assurance", issued by FDA in September 2004<sup>14</sup>, clearly states that suitable Process Analytical Technologies (PAT) have to be used in every manufacturing process of pharmaceutical products, with the goal of evaluating in-line product evolution and, thus, if the desired characteristics are obtained. In the case study of the freeze-drying process, focusing on the primary drying, that is the riskiest step of the whole process due to the higher water content, it is necessary to monitor in-line the following variables:

- i. Product temperature, for the above discussed reasons.
- ii. The residual amount of ice in the product, to identify the ending points of the primary drying stage (thus modifying the operating conditions to promote secondary drying without prolonging unnecessarily the previous step) and of the secondary drying stage (that is identify when the target value of residual moisture has been reached).
- iii. The sublimation flux, that has to be compliant with duct and condenser capacity, for the abovementioned reasons.

Besides, as mathematical modeling may be used for in-line<sup>15-17</sup> or off-line optimization<sup>18-20</sup>, it

can be worthwhile estimating in-line also the values of the parameters of these mathematical models. In particular, the parameters of interest are two, namely  $K_v$ , the heat transfer coefficient between the shelf and the product, and  $R_p$ , the resistance of the dried product to vapor flux.<sup>21</sup> These parameters are used to calculate, respectively, the heat flux to the product ( $J_q$ ) and the sublimation flux ( $J_w$ ):

$$J_q = K_v (T_{shelf} - T_B) \quad (1)$$

$$J_w = \frac{1}{R_p} (p_{w,i} - p_{w,c}) \quad (2)$$

where  $T_{shelf}$  is the temperature of the heating shelf,  $T_B$  is that of the product at the bottom of the container,  $p_{w,i}$  is the solvent partial pressure at the sublimation interface, and  $p_{w,c}$  is that in the drying chamber.

In the last decade several reviews about the available systems for freeze-drying monitoring appeared in the Literature<sup>22-27</sup>. The most recent and up-to-date are those published by the LyoHub consortium<sup>28</sup> and by Fissore et al.<sup>29</sup>. In all these papers a great interest appears towards systems that (i) are able to monitor the whole batch taking into account that the dynamics of the product in the vials, that can be different due to the position of the vial over the shelf<sup>30</sup>, and (ii) that do not interfere with product dynamics. In this framework, i.e. with the goal of monitoring the batch non-invasively, and accounting for its non-uniformity, it is of particular interest the use of plasma sputtered thermocouples embedded into the glass wall<sup>31-33</sup> and of optical fibers with the fiber Bragg gratings embedded in the shelf<sup>34</sup>. Although both systems are effective in reaching previously listed goals, they suffer from relevant drawbacks: (i) they involve using special vials, or (ii) special shelves in the freeze-dryers, and both issues can be hardly compatible with existing apparatus and containers. Hemteborg et al.<sup>34</sup> proposed the use of an infrared camera to monitor product temperature, without any interference with the product, and without using any special vials or special shelves. Unfortunately, in their

arrangement the camera is installed on the top of the freeze-dryer, outside the equipment, and it monitors the product in the vials loaded onto the top shelf, measuring, in particular, the top temperature.

This paper aims at presenting an innovative device consisting of an IR camera that can be placed inside the freeze-dryer, at any position onto the shelves: the system measures the temperature of the glass vials standing in front of it, being product temperature very close to that of the vial wall, as shown by Velardi and Barresi<sup>21</sup>.

The paper is organized in the following way: at first, details about the sensor are given, as well as about the experimental investigation carried out; then, main results are presented and discussed, focusing on the effect of the insertion of the sensor in the chamber on product dynamics, the validation of the measurements of product temperature and the estimates of the ending point of the primary drying and of the model parameters  $K_v$  and  $R_p$ .

## **Materials and methods**

### *IR camera*

Monitoring of product temperature was carried out by a specially designed system (IMC Service S.r.l., Italy), composed of the following elements (Figure 1);

- A thermal camera (FILR Systems model A35);
- A standard video camera;
- A cold LED illuminator;
- A processing board, i.e. hardware/software system designed for the management of all components, without the need for an external computer, and WiFi communication;
- A status LED, that allows to know the status of TICEM;

- A couple of special valves designed to allow the system to be flushed with nitrogen or other gases.

As the system was aimed to be placed in the drying chamber, the following issues had to be addressed:

- The impact of the operating conditions throughout the freeze-drying process;
- The measurement accuracy;
- The attainment of an autonomous operation mode and data access.

The freeze-drying chamber, during the cycle, is characterized by low temperature, up to -40/-50°C in the freezing stage, low pressure and a gas composition about 100% water vapor. The optimization of the thermal insulation of the existing container was discarded, because of the size of the case and of several problems in the management of data transfer, and the design of a protective enclosure in a thermally insulating plastic material, transparent to WiFi communications, was preferred. The preventive filling of the case with nitrogen was required to avoid the onset of halos due to the condensation of any humidity present inside the case.

The accuracy of a temperature measurement obtained with a thermal imaging camera involves the knowledge of several parameters in order to "correct" the influence of parasitic radiations and process the data coming from the measured system. In the specific case, the key parameters are the followings:

- Emissivity of the subject;
- Distance from the subject;
- Reflected apparent temperature;
- Room temperature and humidity.

The emissivity of the measured element, as well as its distance from the camera, can be easily calculated and fixed for the whole duration of the test. The ISO 18434-1<sup>36</sup> guideline (Part 1, Annex A.2) was used to this purpose: the temperature of glass vials was increased, through



external heating, until it was 20°C higher than that of the environment where the vials were placed, and the emissivity was estimated. The test was repeated considering, as starting temperature, different values in the typical range of a freeze-drying process, namely from -40°C to +20°C, and a mean value of 0.9 was obtained for glass emissivity.

With respect to room temperature and humidity, using a mean value estimated from the values usually occurring in a freeze-drying process, a maximum error of 0.01°C is expected in the measured temperature and, thus, both values were not optimized.

On the contrary, the reflected apparent temperature has much more importance. The term "reflected apparent temperature" refers to the set of radiations that the surrounding environment emits towards the measured item, and that the same "reflects" towards the thermal camera together with its own radiation. The estimation of this parameter has a dramatic effect on the measurement, leading to errors of several tens of degrees depending on the material measured. Unfortunately, during a freeze-drying cycle, the surrounding environment considerably changes the amount of radiation emitted towards the measured items (cooling - drying - heating) and, therefore, it is particularly difficult to identify the correct value to be entered manually. During the setup of the instrumentation various tests were carried out using external probes to read the temperature in a known area and/or with the adoption of different mean values of the reflected apparent temperature. The solution that allowed to obtain a reliable result for the whole duration of the process was to use an area of the framed field as "pure reflector" and read the value of the "apparent temperature" reflected with the thermal camera (according to ISO 18434-1<sup>36</sup> guideline, Part 1, Annex A.1). The software was customized to measure and update this variable in-line automatically.

Finally, the system was designed to operate in the absence of external terminals: the software architecture of the system provides a main core for the management of connections with the instrumentation and the work sessions, a communication core for the management of

external users, the transmission of commands, and the configurations to the main core. The user may connect to the system via WiFi when necessary, displaying in real time the data of the current session (if active), or accessing the archive to download the sessions already completed.

### *Case study*

Freeze-drying tests were carried out using a LyoBeta 25™ (Telstar, Spain) freeze-dryer (drying chamber: 0.2 m<sup>3</sup>, total area: 0.5 m<sup>2</sup>). Most of the tests were carried out processing a 10% by weight sucrose solution, although also the processing of a 5% by weight sucrose solution was considered for validation purposes. Reactants were purchased from Sigma Aldrich and used as received; ultra-pure water obtained with a Millipore water system (Milli-Q RG, Millipore, Billerica, MA) was used to prepare the solutions processed in the various tests. In all tests glass vials (ISO 8362-1 10R) were filled with 5 ml of solution and placed directly on the shelf: the distance of the first row from the camera was 30 cm, and a new image was acquired every five minutes.

Thin T-type thermocouples (Tersid, Italy) were placed in some vials for validation purposes. Chamber pressure was monitored using both a capacitance (Baratron type 626A, MKS Instruments, USA) and a thermal conductivity (Pirani type PSG-101-S, Inficon, Switzerland) gauge, being the ratio of the two signals used to identify the ending point of the primary drying stage<sup>37</sup>.

Product freezing was achieved by decreasing the temperature of the technical fluid at about 1°C/min, until a temperature of about -40°C was reached by the product. Then, the operating conditions of the freeze-drying process were set according to the specific goal of the test, as discussed in the following section. All the drying tests was carried out in non-GMP conditions.

## Results and discussion

### *Study of the effect of the presence of the IR camera on the batch evolution*

The first set of tests was carried out to assess the effect of the presence of the IR camera on the dynamics of the vials of the batch. In all the tests the same values of temperature of the heating shelf and of the pressure in the drying chamber were used:  $-20^{\circ}\text{C}$  and 20 Pa respectively. As it will be shown in the following, when the values of product temperature during primary drying, as well as those of dried cake resistance to vapor flux, will be shown and discussed, these operating conditions resulted in the microscopic collapse of the dried cake, a small-scale collapse resulting in the formation of small holes in the dried cake and, thus, in the reduction of cake resistance.<sup>38,39</sup> In any case, considering the goals of the study, i.e. to assess the effect of the IR camera on product dynamics and validating the temperature values obtained through this device, the selected operating conditions are irrelevant.

In the first test 10 vials were loaded onto one of the shelves of the freeze-dryer, arranged in one row, without the infrared camera, while in the second test the IR camera was introduced in the drying chamber, as shown in Figure 2. The mass of each vial was measured before starting the freeze-drying process, and after 5 hours from the onset of the primary drying stage. Considering the two vials exactly in front of the camera, the weight loss is 2.62 g and 2.73 g in test #1, while the values obtained in test #2 are 1.47 g and 1.49 g. This seems to suggest that the presence of the camera in the drying chamber has a shielding effect from radiation on the vials standing in front of it. An additional test was carried out, loading 45 vials onto one of the shelves of the freeze-dryer, arranged in three rows of 15 vials, without the thermal camera: row 1 faces the wall of the chamber, while row 3 faces the door of the chamber (Figure 3). The mass of each vial was measured before starting the freeze-drying process and after 5 hours from the

onset of the primary drying stage. The values of weight loss in each vial are shown in Table 1. It appears that the mean weight loss in the central vials is 1.04 g (with a standard deviation of 7.92%), while in the edge vials we get 1.54 g (with a standard deviation of 12.04%), corresponding to a sublimation flux of  $0.83 \text{ kg h}^{-1}\text{m}^{-2}$  and  $1.16 \text{ kg h}^{-1}\text{m}^{-2}$  respectively. The same test was repeated introducing the infrared camera in the drying chamber in such a way that it monitors directly vials of row 1 and, in particular, vials #2 to #13. The values of weight loss are shown in Table 2. The mean weight loss in the central vials is 1.09 g, while in the edge vials we get 1.37 g, corresponding to a sublimation flux of  $0.85 \text{ kg h}^{-1}\text{m}^{-2}$  and  $1.06 \text{ kg h}^{-1}\text{m}^{-2}$  respectively. Evaluating the standard deviation of the weight loss in the edge vials a quite large value is obtained, 22.7%, thus suggesting a certain degree of non-uniformity among the dynamics exhibited by the vials of the batch. Therefore, we focused on the weight loss of the vials facing the IR camera, i.e. those from vials #2 to #13, excluding vials #9 and #10 as they are placed in front of the cold LED. The mean weight loss in these containers is 1.17 g (with a standard deviation of 3.0%), while in the other vials of row number 1 the mean weight loss is 1.63 g. Therefore, it appears that the weight loss in the vials standing in front of the IR camera is very close to the value obtained for the central vials (just 7% higher, while without the IR camera the weight loss in the same vials is 30% higher than that of the central vials). This result seems to suggest that the IR camera acts as a sort of shield for the vials of the row standing in front of it, whose dynamics is thus very close to that of central vials, while the effect is poor for the others. This is of outmost importance as when we use the IR camera in the freeze-dryer we are obviously able to monitor the evolution of the temperature only in the row of vials facing the camera, and not that of central vials, that are the majority of the batch. Anyway, as it appears that the dynamics of the product in the vials standing exactly in front of the camera is similar to that of the vials in the center of the batch, while the dynamics of the other vials of the row is still that of the edge vials, then the IR camera can be used to effectively monitor the whole batch

being processed.

#### *Validation of the monitoring system based on the IR camera: temperature measurement*

The first step of the validation of the monitoring system based on the use of the IR camera in the freeze-dryer was focused on the comparison between the temperature measured through thermocouples inserted in some vials of the batch, and the values measured through the IR camera. An example of thermography obtained in one of these tests is shown in Figure 4. In the top picture the two thermocouples inserted in two different vials can be easily detected, but it is not possible to identify the tip of the sensor, as it is immersed into the product, and, thus, which is the point whose temperature is measured. The IR camera provides the temperature distribution in all the vials, where it is well known that the temperature is not uniform both in the radial direction, due to the effect of radial heating from the vial wall, and in the axial direction, due to the heat conduction in the frozen and in the dried product. Therefore, just for comparison purposes, the temperature evolution detected by the IR camera in five points in different positions (shown in Figure 4, bottom picture), close to the bottom of the vial, was considered, and compared to the temperature profile detected by the thermocouple (in the same monitored vial). Results are shown in Figure 5, evidencing that the difference between the temperature values detected by the thermocouple and by the IR camera at the bottom of the product is very small, and is comprised in the uncertainty range of thermocouple measurements ( $\pm 1^{\circ}\text{C}$ ). Similar comparisons were carried out in other cases studies, modifying the operating conditions and the type of product (not shown in this paper for sake of brevity), namely aqueous solutions containing sucrose at different concentrations (5% and 10%), or mannitol (at the same concentration), as they are representative, respectively, of amorphous and crystalline products, and a similar agreement was always observed.

#### *Validation of the monitoring system based on the IR camera: end of primary drying estimation*

The temperature profile detected through a thermocouple can be used to infer the ending point of the primary drying stage<sup>37</sup>. In fact, the temperature of the product is a consequence of the heat transferred by the freeze-dryer to the product in the vial, and of the heat subtracted from the product as it is used for ice sublimation. In a freeze-drying process, at the beginning of the primary drying stage product temperature increases from the value reached at the end of the freezing stage till a value corresponding to a sort of steady-state, where all the heat transferred to the product is used for the ice sublimation and, thus, product temperature does not change. This takes place in all those cases where resistance of the dried product to vapor flow remains almost constant throughout the primary drying stage (apart from the initial rise, obviously), e.g. when the product is freeze-dried slightly above its microscopic collapse temperature. In other cases, when the resistance of the dried cake increases a lot as drying goes on, also product temperature continuously increases during the primary drying stage. When the ice sublimation is completed, product temperature increases further up to the thermal equilibrium with the environment, that is the shelf and eventual radiation from the surroundings. Figure 6, top graph, compares the mean temperature detected at the bottom of the product by the IR camera and the pressure ratio, that is usually used to assess the ending point of the main drying, when the 10% sucrose solution is processed. It is possible to see that both curves reach the final asymptote at the same time, about 35 hours. A similar trend is observed in Figure 6, bottom graph, where the results obtained when processing the 5% sucrose solution are shown. These results prove that the mean temperature detected using the IR camera can be successfully used to detect the ending point of the primary drying stage, at least with the same uncertainty of the pressure ratio.

#### *Validation of the monitoring system based on the IR camera: $K_v$ and $R_p$ estimation*

Finally, the temperature detected by the IR camera can be used to estimate the values of the

heat and mass transfer coefficients  $K_v$  and  $R_p$ , defined in equations (1) and (2), as it can be done using the temperature measurement obtained through a thermocouple (details of the algorithm, not shown here for sake of brevity, are given in Ref.<sup>40</sup>). The test was carried out processing the 10% sucrose solution and measuring product temperature with both a thermocouple and the IR camera in the freeze-dryer. The test was repeated 5 times and when considering the thermocouple measurements, the mean value of  $K_v$  obtained was  $156.5 \text{ W m}^{-2}\text{K}^{-1}$  (with a standard deviation of 8.65%). Using the mean bottom temperature detected by the IR camera, the mean value of  $K_v$  obtained was  $153.0 \text{ W m}^{-2}\text{K}^{-1}$  (with a standard deviation of 12.33%), thus in perfect agreement with the previous value. The quite high value of  $K_v$  obtained is a consequence of the peculiar arrangement of the vials in these tests, as just one row of vials in considered and, thus, radiation from chamber walls plays a great role in product heating; besides, also the value of chamber pressure, 20 Pa, is responsible for a higher value of  $K_v$ .

With respect to the coefficient  $R_p$ , it can be calculated using the temperature profile (detected through the thermocouple or the IR camera) and the  $K_v$  value. From the value of  $K_v$  and that of the temperatures of the heating shelf and of the product at the bottom of the vial, it is possible to calculate the heat flux to the product using eq. (1). Then, considering the following heat balance to the product:

$$J_q = \Delta H_s J_w \quad (3)$$

stating that all the heat transferred to the product is used for ice sublimation, the water vapor flux can be easily calculated and, finally, the value of  $R_p$  using eq. (2), as  $p_{w,c}$  may be assumed to be equal to chamber pressure (being the composition of the atmosphere in the chamber about 100% water vapor), and  $p_{w,i}$  a well-known function of product temperature (details of the calculations are given in Ref.<sup>40</sup>). Figure 7, top graph, shows the values of  $R_p$  as a function of the thickness of the dried layer as they are calculated from the measurement of product temperature through a thermocouple. These values are interpolated using the following

equation:

$$R_p = R_{p,0} + \frac{AL_{dried}}{1 + BL_{dried}} \quad (4)$$

that is quite often used to express the dependence of the resistance of the dried product on its thickness. Figure 7, bottom graph, shows the values of  $R_p$  obtained using the mean value of product temperature at the bottom of the vial, as detected by the IR camera, and the mean value of  $K_v$  previously obtained, as well as the two curves of  $R_p$  vs  $L_{dried}$  obtained considering the standard deviation of the values computed for  $K_v$ . Also in this case it is possible to point out an acceptable agreement between the values of  $R_p$  vs  $L_{dried}$  obtained using the thermocouple measurement and the IR camera outcomes.

## Conclusions

The IR camera presented in this paper stands out as a unique system able to on-line monitor a freeze-drying process, without interfering with product dynamics and providing information not only about product temperature, but also about the ending point of the primary drying stage, and about the coefficients  $K_v$  and  $R_p$ . The accuracy about the measurements and the estimates obtained with this system appears to be similar to that typical of a traditional thermocouple, but in this case the sensor is not in contact with the product, and the measure is not limited to a single vial. It has to be remarked that although through the IR camera it is possible to monitor only the first row of vials of the batch, the camera shields the vials standing in front of it from wall radiation and, thus, the sublimation flux in those vials is similar to that of the “central” vials of the batch. This means that monitored vials are representative of most of the vials of the batch.

Future investigations will deal with the use of multivariate image analysis, i.e. statistical



tools, to infer as much information as possible from the obtained thermography and for classification purposes, that is process monitoring and fault detection.

## List of symbols

$A$	parameter used to express the dependence of $R_p$ on $L_{dried}$ , $s^{-1}$
$B$	parameter used to express the dependence of $R_p$ on $L_{dried}$ , $m^{-1}$
$\Delta H_s$	heat of sublimation, $J\ kg^{-1}$
$J_q$	heat flux to the product, $W\ m^{-2}$
$J_w$	mass flux, $kg\ s^{-1}m^{-2}$
$K_v$	overall heat transfer coefficient between the heating fluid and the product at the vial bottom, $W\ m^{-2}K^{-1}$
$L_{dried}$	thickness of the dried layer, $m$
$p_{w,c}$	water vapor partial pressure in the drying chamber, $Pa$
$p_{w,i}$	water vapor partial pressure at the interface of sublimation, $Pa$
$R_p$	resistance of the dried product, $m\ s^{-1}$
$R_{p,0}$	parameter used to express the dependence of $R_p$ on $L_{dried}$ , $m\ s^{-1}$
$T_B$	product temperature at the vial bottom, $K$
$T_{shelf}$	heating shelf temperature, $K$

## List of references

1. Mellor JD, 1978. Fundamentals of freeze-drying. Academic Press, London.
2. Jennings TA, 1999. Lyophilization: introduction and basic principles. Interpharm/CRC Press, Boca Raton.
3. Oetjen GW, Haseley P, 2004. Freeze-Drying. Wiley-VHC. Weinheim.
4. Fissore D, 2013. Freeze-drying of pharmaceuticals, in: Swarbrick J (Ed.), Encyclopedia of Pharmaceutical Science and Technology, 4th Edition. CRC Press, London, pp. 1723-1737.
5. Pikal MJ, Shah S, Roy ML, Putman R. The secondary drying stage of freeze drying: drying kinetics as a function of temperature and chamber pressure. *Int J Pharm* 1990;60(3):203-207.
6. Bellows RJ, King CJ. Freeze-drying of aqueous solutions: Maximum allowable operating temperature. *Cryobiology* 1972;9(6):559-561.
7. Tsourouflis S, Flink JM, Karel M. Loss of structure in freeze-dried carbohydrates solutions: effect of temperature, moisture content and composition. *J. Sci. Food Agric.* 1976;27(6):509-519.
8. Adams GDJ, Irons LI. Some implications of structural collapse during freeze-drying using *Erwinia caratovora* Lasparaginase as a model. *J. Chem. Tech. Biotech.* 1993;58(1):71-76.
9. Pikal MJ, 1994. Freeze-drying of proteins: Process, formulation, and stability, in Cleland JL, Langer R, (Eds.), Formulation and Delivery of Proteins and Peptides. American Chemical Society, Washington, pp. 120-133.
10. Franks F. Freeze-drying of bioproducts: putting principles into practice. *Eur. J. Pharm. Biopharm.* 1998;45(3):221-229.
11. Wang DQ, Hey JM, Nail SL. Effect of collapse on the stability of freeze-dried recombinant factor VIII and  $\alpha$ -amylase. *J. Pharm. Sci.* 2004;93(5):1253-1263.

12. Searles J. Observation and implications of sonic water vapour flow during freeze-drying. *Am. Pharm. Rev.* 2004;7(2):58-69.
13. Patel SM, Swetaprovo C, Pikal MJ. Choked flow and importance of Mach I in freeze-drying process design. *Chem. Eng. Sci.* 2010;65(21):5716-5727.
14. Food and Drug Administration. Guidance for Industry PAT - A Framework for Innovative Pharmaceutical Manufacturing and Quality Assurance, 2004. <https://www.fda.gov/downloads/drugs/guidances/ucm070305.pdf> (last access: June 2018).
15. Pisano R, Fissore D, Velardi SA, Barresi AA. In-line optimization and control of an industrial freeze-drying process for pharmaceuticals. *J. Pharm. Sci.* 2010;99(11):4691-4709.
16. Daraoui N, Dufour P, Hammouri H, Hottot A. Model predictive control during the primary drying stage of lyophilisation. *Contr. Eng. Pract.* 2010;18(5):483-494.
17. Pisano R, Fissore D, Barresi AA. Freeze-drying cycle optimization using Model Predictive Control techniques. *Ind. Eng. Chem. Res.* 2011;50(12):7363-7379.
18. Giordano A, Barresi AA, Fissore D. On the use of mathematical models to build the design space for the primary drying phase of a pharmaceutical lyophilization process. *J. Pharm. Sci.* 2011;100(1):311-324.
19. Fissore D, Pisano R, Barresi AA. Advanced approach to build the design space for the primary drying of a pharmaceutical freeze-drying process. *J. Pharm. Sci.* 2011;100(11):4922-4933.
20. Koganti VR, Shalaev EY, Berry MR, Osterberg T, Youssef M, Hiebert DN, Kanka FA, Nolan M, Barrett R, Scalzo G, Fitzpatrick G, Fitzgibbon N, Luthra S, Zhang L. Investigation of design space for freeze-drying: Use of modeling for primary drying segment of a freeze-drying cycle. *AAPS PharmSciTech* 2011;12(3):854-861.
21. Velardi SA, Barresi AA. Development of simplified models for the freeze-drying process

- and investigation of the optimal operating conditions. *Chem. Eng. Res. Des.* 2008;86(1):9-22.
22. Barresi AA, Pisano R, Fissore D, Rasetto V, Velardi SA, Vallan A, Parvis M, Galan M. Monitoring of the primary drying of a lyophilization process in vials. *Chem. Eng. Proc.* 2009;48(1):408-423.
  23. Johnson RE, Gieseler H, Teagarden DL, Lewis LM. Analytical accessories for formulation and process development in freeze-drying. *Am. Pharm. Rev.* 2009;12(5):54-60.
  24. Wiggenhorn M, Winter G, Presser I. The current state of PAT in freeze-drying. *Am. Pharm. Rev.* 2005;8(1):38-44. *Eur. Pharm. Rev.* 2005;10(4):87-92.
  25. Patel SM, Pikal MJ. Process Analytical Technologies (PAT) in freeze-drying of parenteral products. *Pharm. Dev. Tech.* 2009;14(6):567-587.
  26. Patel SM, Doen T, Pikal MJ. Determination of the end point of primary drying in freeze-drying process control. *AAPS PharmSciTech* 2010;11(1):73-84.
  27. Barresi AA, Fissore D, 2011. In-line product quality control of pharmaceuticals in freeze-drying processes, in Tsotsas E, Mujumdar AS, (Eds.), *Modern Drying Technology Vol. 3: Product Quality and Formulation*. Wiley-VCH Verlag GmbH & Co. KGaA, Weinheim, pp. 91-154.
  28. Nail S, Tchessalov S, Shalaev E, Ganguly A, Renzi E, Dimarco F, Wegiel L, Ferris S, Kessler W, Pikal M, Sacha G, Alexeenko A, Thompson TN, Reiter C, Searles J, Coiteux P. Recommended best practices for process monitoring instrumentation in pharmaceutical freeze drying-2017. *AAPS PharmSciTech* 2017;18(7):2379-2393.
  29. Fissore D., Pisano R, Barresi AA. Process analytical technology for monitoring pharmaceuticals freeze-drying – A comprehensive review. *Drying Technol.* In press (DOI: 10.1080/07373937.2018.1440590).
  30. Barresi AA, Pisano R, Rasetto V, Fissore D, Marchisio DL. Model-based monitoring and

- control of industrial freeze-drying processes: Effect of batch non-uniformity. *Drying Technol.* 2010;28(5):577-590.
31. Parvis M, Grassini S, Barresi A. Sputtered thermocouple for lyophilization monitoring. In Proceedings of IEEE International Instrumentation and Measurement Technology Conference "I2MTC 2012", Graz, Austria, May 13-16, 2012; 1994-1998 (Paper 1569530153).
  32. Grassini S, Parvis M, Barresi AA. Inert thermocouple with nanometric thickness for lyophilization monitoring. *IEEE Trans. Inst. Meas.* 2013;62(5):1276-1283.
  33. Parvis M, Grassini S, Fulginiti D, Pisano R, Barresi AA. Sputtered thermocouple array for vial temperature mapping. In Proceedings of IEEE International Instrumentation and Measurements Technology Conference "I2MTC 2014", Montevideo, Uruguay, May 12-15, 1465-1470, 2014.
  34. Kasper JC, Wiggenhorn M, Resch M, Friess W. Implementation and evaluation of an optical fiber system as novel process monitoring tool during lyophilization. *Eur. J. Pharm. Biopharm.* 2013;83(3):449-459.
  35. Hemteborg H, Zeleny R, Charoud-Got J, Martos G, Luddeke J, Schellin H, Teipel K. Infrared thermography for monitoring of freeze-drying processes: instrumental developments and preliminary results. *J. Pharm. Sci.* 2014;103(7):2088-2097.
  36. International Standard ISO 18434-1, 2008. Condition monitoring and diagnostics of machines - Thermography - Part 1: General procedures. <https://www.iso.org/obp/ui/#iso:std:iso:18434:-1:ed-1:v1:en> (last access date: June 2018)
  37. Patel SM, Doen T, Pikal MJ. Determination of end point of primary drying in freeze-drying process control. *AAPS PharmSciTech* 2010;11:73-84.
  38. Overcashier DE, Patapoff TW, Hsu CC. Lyophilization of protein formulations in vials: Investigation of the relationship between resistance to vapor flow during primary drying

and small-scale product collapse. *J Pharm Sci* 1999;99(7):688-695.

39. Kuu WY, O'Bryan KR, Hardwick LM, Paul TW. Product mass transfer resistance directly determined during freeze-drying cycle runs using tunable diode laser absorption spectroscopy (TDLAS) and pore diffusion model. *Pharm Dev Technol.* 2011;16(4):343-357.
40. Fissore D, Pisano R, Barresi AA. On the use of temperature measurement to monitor a freeze-drying process for pharmaceuticals. In Proceedings of IEEE International Instrumentation and Measurements Technology Conference "I2MTC 2017", Torino, Italy, May 22-25, 1276-1281, 2017.

## List of Tables

**Table 1.** Values of weight loss, in grams, in each vial at the end of the test without the thermal camera in the freeze-dryer.

**Table 2.** Values of weight loss, in grams, in each vial at the end of the test with the thermal camera in the freeze-dryer.



## List of Figures

**Figure 1.** Sketch of the IR thermal camera used in this study (1: thermal camera, 2: rgb camera, 3: cold led, 4: connections to a gaseous stream, 5: status led).

**Figure 2.** Freeze-dryer chamber with the vial arrangement used in the tests aiming to assess the effect of the presence of the IR camera on product drying.

**Figure 3.** Sketch of the vial arrangement used in test #3.

**Figure 4.** Top picture: thermography obtained during a freeze-drying cycle. Bottom picture: detail of the vials, with the five points used to track the evolution of product temperature.

**Figure 5.** Comparison between the temperature detected in the five points at the bottom of the vial, as illustrated in Figure 4, (lines) and the measurement of a thermocouple (symbols) placed in the same vial. Case study: freeze-drying of a 10% w/w sucrose solution, processed at 20 Pa and -20°C.

**Figure 6.** Comparison between the mean value of product temperature (dashed line) detected through the IR thermal camera in the five points at the bottom of the vial and the ratio between the Pirani and Baratron signals (solid line) when processing a 10% (top graph) or a 5% (bottom graph) w/w sucrose solution at 20 Pa and -20°C.

**Figure 7.** Comparison between the values of resistance of the dried cake to vapor flux *vs* thickness of the dried product calculated using the thermocouples measurements, black squares

(top graph), and using the IR thermography, black triangles, bottom graph. Solid lines correspond to the trend calculated using eq. (4), while dashed lines are the trends calculated taking into account the uncertainty on the overall heat transfer coefficient  $K_v$ .

Table 1

	Position														
	1	2	3	4	5	6	7	8	9	10	11	12	13	14	15
Row 1	1.67	1.66	1.51	1.43	1.32	1.26	1.25	1.26	1.14	1.36	1.26	1.3	1.34	1.46	1.59
Row 2	1.46	1.16	1.06	0.82	1.13	1.02	1.01	0.99	1.08	1.08	1.08	1.04	1.02	1.01	1.42
Row 3	1.6	1.93	1.45	1.36	1.29	1.34	1.44	1.41	1.39	1.86	1.42	1.41	1.48	1.55	1.63

Table 2

	Position														
	1	2	3	4	5	6	7	8	9	10	11	12	13	14	15
Row 1	1.55	1.2	1.17	1.12	1.16	1.21	1.11	1.16	1.33	1.48	1.21	1.2	1.18	2.2	1.15
Row 2	1.21	0.98	0.96	0.96	0.95	1.22	1.12	0.98	1.09	1.54	1.08	0.89	0.97	1.46	1.38
Row 3	1.53	1.19	1.14	1.13	1.24	1.93	1.39	1.18	1.62	1.57	0.91	1.14	1.86	2.03	1.8

*Figure 1*

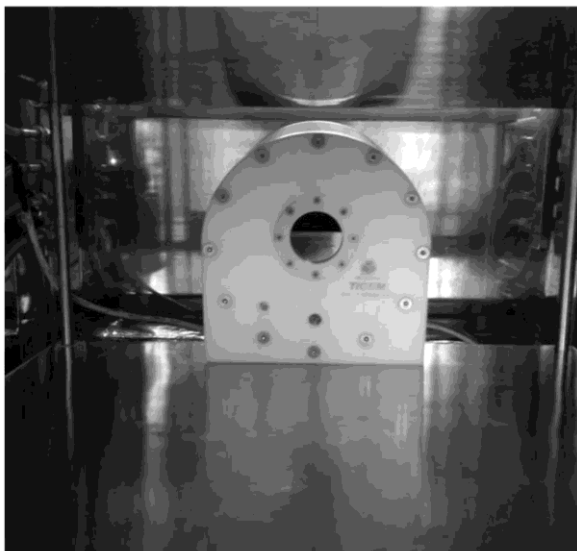
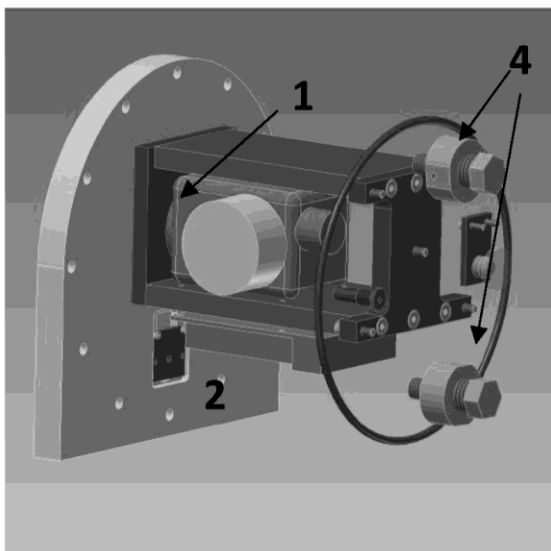
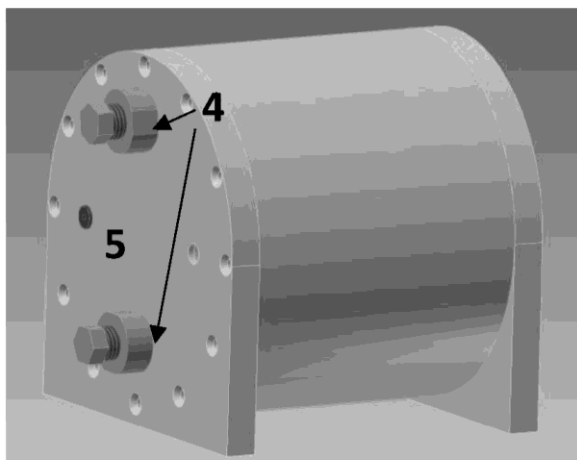
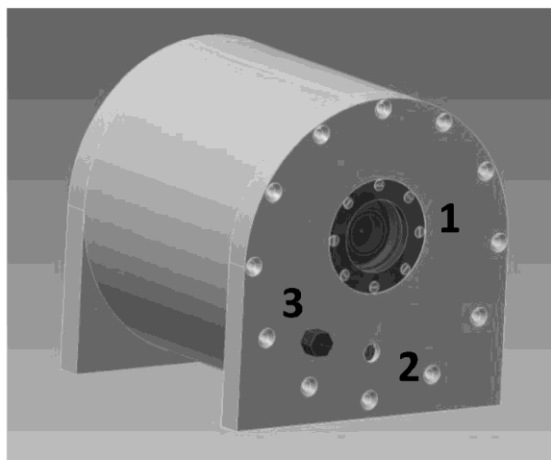


*Figure 2*

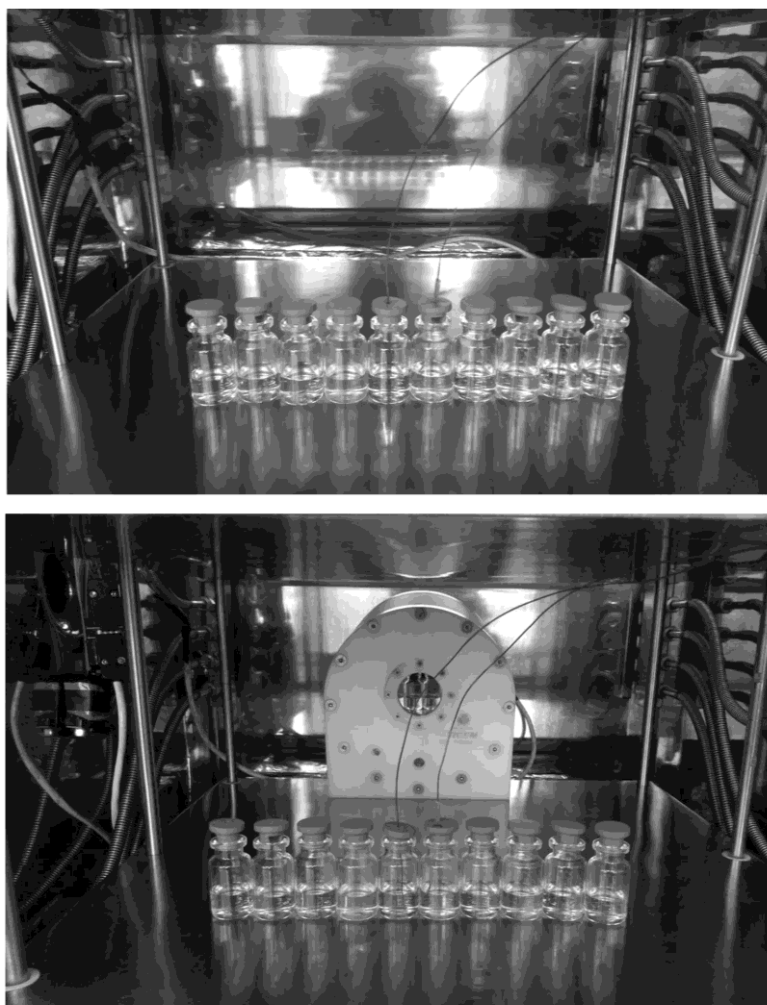
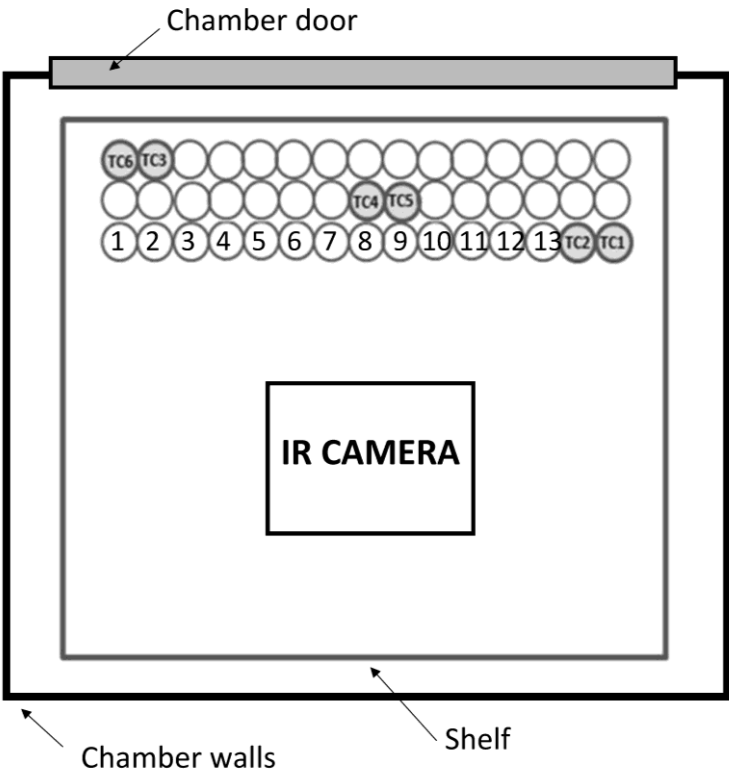


Figure 3



*Figure 4*

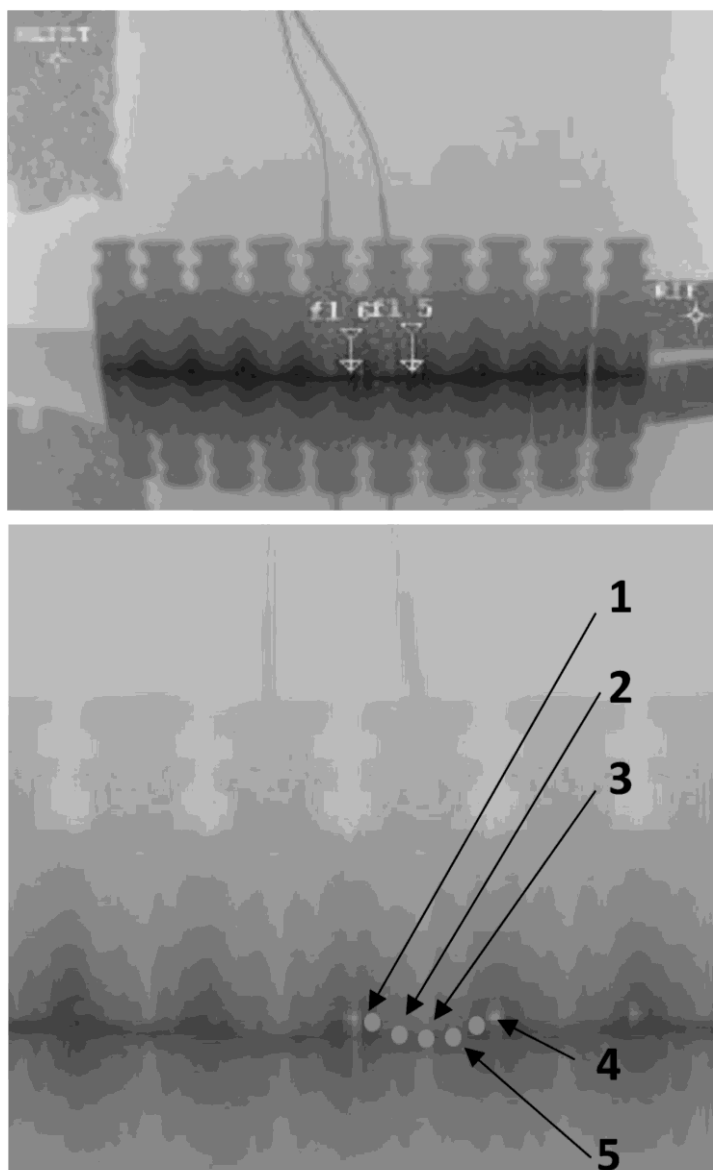




Figure 5

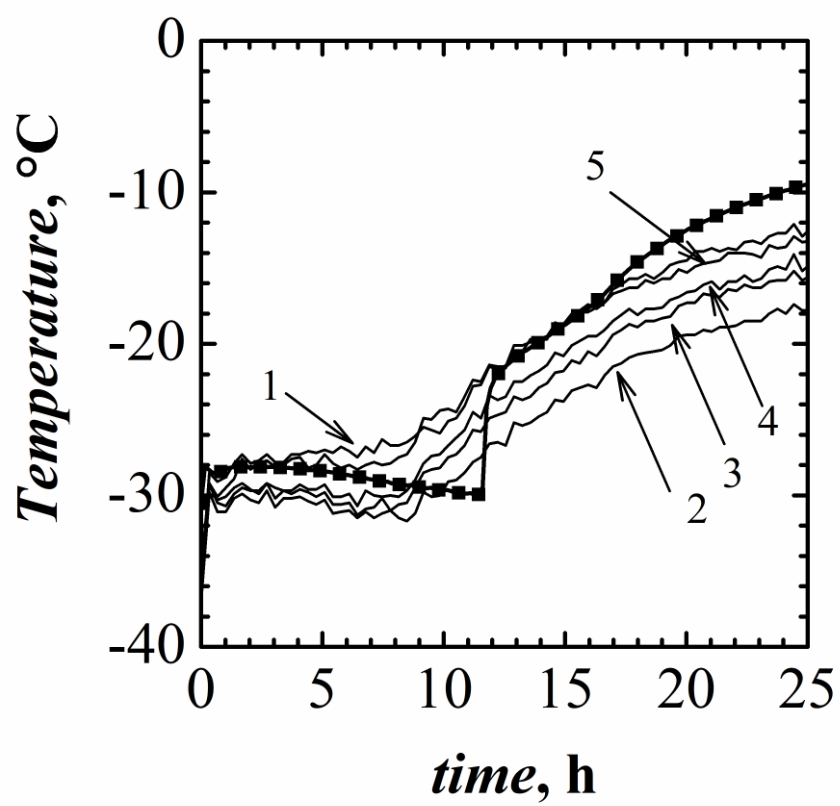


Figure 6

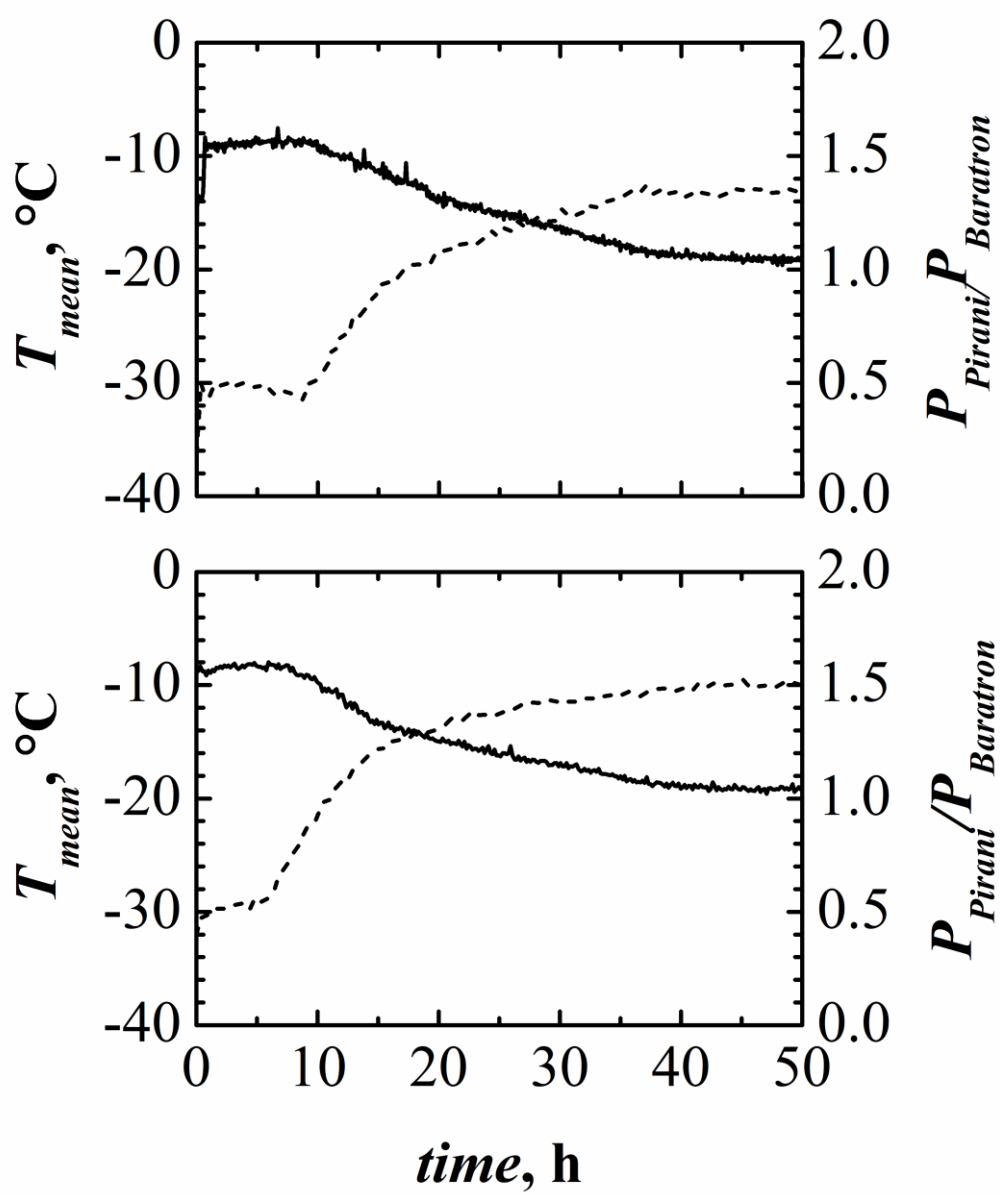


Figure 7

